Estrogen receptor α promotes breast cancer by reprogramming choline metabolism

Min Jia[1], Trygve Andreassen[2], Lasse Jensen[3, 4], Tone Frost Bathen[5], Indranil Sinha[1], Hui Gao[1], Chunyan Zhao[1], Lars-Arne Haldosen[1], Yihai Cao[3], Leonard Girnita[6], Siver Andreas Moestue[5], Karin Dahlman-Wright[1]

[1]Department of Biosciences and Nutrition, Novum, Karolinska Institutet, 141 83 Huddinge, Sweden; [2]MR Core Facility, Department of Circulation and Medical Imaging, Norwegian University of Science and Technology, N-7489 Trondheim, Norway; [3]Department of Microbiology, Tumor, and Cell Biology, Karolinska Institutet, 171 77 Stockholm, Sweden; [4]Unit of Cardiovascular Medicine, Department of Medical and Health Sciences, Linköping University, 581 83 Linköping, Sweden; [5] Department of Circulation and Medical Imaging, Norwegian University of Science and Technology, N-7489 Trondheim, Norway; [6]Department of Oncology and Pathology, Karolinska Institutet and Karolinska University Hospital, 17176 Stockholm, Sweden.

Corresponding Author

Min Jia, Department of Biosciences and Nutrition, Novum, Karolinska Institute, S-141 83 Huddinge, Sweden. Phone: 46-8-52481221; Fax: 46-8-52481130; E-mail: min.jia@ki.se; and Karin Dahlman-Wright, Department of Biosciences and Nutrition, Novum, Karolinska Institute, S-141 83 Huddinge, Sweden. E-mail: Karin.Dahlman-Wright@ki.se

Running title: ERα reprogramms cell metabolism

Keywords: Estrogen receptor α; breast cancer; chromatin; metabolism; transcription

Word count: 4506

Total number of figures and tables: 7 figures

Disclosure: The authors declare no conflicts of interest.

Abstract

Estrogen receptor α (ERα) is a key regulator of breast growth and breast cancer development. Here we report how ERα impacts these processes by reprogramming metabolism in malignant breast cells. We employed an integrated approach, combining genome-wide mapping of chromatin-bound ERα with estrogen-induced transcript and metabolic profiling, to demonstrate that ERα reprograms metabolism upon estrogen stimulation, including changes in aerobic glycolysis, nucleotide and amino acid synthesis and choline (Cho) metabolism. Cho phosphotransferase CHPT1, identified as a direct ERα-regulated gene, was required for estrogen-induced effects on Cho metabolism including increased phosphatidylcholine (PtdCho) synthesis. CHPT1 silencing inhibited anchorage-independent growth and cell proliferation, also suppressing early-stage metastasis of tamoxifen (TMX)-resistant breast cancer cells in a zebrafish xenograft model. Our results showed that ERα promotes metabolic alterations in breast cancer cells mediated by its target CHPT1, which this study implicates as a candidate therapeutic target.

Introduction

Complementary to viewing cancer as a genetic disease, cancer can be considered a metabolic disease (1,2). Altered metabolism in cancer directs enhanced nutrient acquisition and facilitates assimilation of carbon into macromolecules such as lipids, proteins and nucleic acids. The net effect of these activities is to support cell growth and proliferation (3-6).

17β-estradiol (E2) and its receptor estrogen receptor α (ERα) have been implicated in promoting proliferation, survival, and migration of breast cancer cells through multiple mechanisms thereby contributing to tumor growth and progression (7,8). Individuals with ERα positive (ERα+) breast cancer as determined by immunohistochemistry (IHC), accounts for approximately 70% of breast cancer patients. Comparative metabolomics profiling of ERα+ and ERα negative (ERα-) breast cancer indicated clear metabolic differences correlated to hormone receptor status, including differences in glutamine and beta-alanine metabolism, as well as phospholipid metabolism (9-11). Furthermore, estrogen stimulation enhanced the rate of glucose consumption, lactate production (aerobic glycolysis), and glutamate synthesis, and decreased the level of phosphocholine (PCho) in breast cancer cell lines (12-14).

Choline (Cho) is an essential nutrient that is necessary for cell membrane synthesis and functions as an important methyl donor (15,16). Routing of Cho through its various metabolic pathways is cell and tissue specific (17). Following uptake of Cho, the intracellular metabolism of Cho is partitioned along two major pathways: (a) converted to PCho for the synthesis of phosphatidylcholine (PtdCho), a major constituent of cell membranes; or (b) oxidation to produce the methyl donor betaine (16). Abnormally high synthesis of PtdCho via the cytidine diphosphate-choline (CDP-Cho) pathway, where CTP:phosphocholine cytidylyltransferase (CCT) has been identified as the rate-limiting enzyme, is generally recognized as a metabolic hallmark of cancer (18,19). PtdCho can also be synthesized through

methylation of phosphatidylethanolamine (PE) by phosphatidylethanolamine N-methyltransferase (PEMT) (20). The *PEMT* gene has been shown to be induced by estrogen in hepatocytes (20).

Increased levels of PCho and total Cho-containing metabolites have been identified as markers for breast cancer (21). Furthermore, increased synthesis of PtdCho is one of the earliest metabolic events associated with the initial stimulation of cell growth and proliferation by tumor promoters in normal cells (22-24). PtdCho has also been found to be increased in breast cancer cells by tumor promoter (25). Consistently, human breast cancer cells have been shown to have higher levels of PtdCho than normal human mammary epithelial cells (26). Underlying mechanisms and potential drug targets in abnormal Cho phospholipid metabolism have been widely investigated in different cancers as reviewed in (19). Overall, the regulation of Cho phospholipid metabolism in breast cancer cells has been shown to depend on breast cancer subtype with respect to gene expression profiles and metabolic fingerprints (27).

Several studies have provided important insights into global estrogen regulated gene networks based on profiling ERα binding regions and estrogen regulated expression (28-33). To extend global estrogen regulated networks to effects on breast cancer metabolism, we report a comprehensive analysis of estrogen regulated metabolic pathways in two breast cancer cell lines. We integrate cistrome, transcriptome and metabolome data to identify metabolic pathways regulated by estrogen signaling via ERα. We focus on effects conserved between two ERα+ breast cancer cell lines with the aim to identify general effectors of metabolic signaling rather than cell type specific effects.

Materials and Methods

Additional and detailed methods are included in the supplementary materials and methods.

Cell culture

MCF7 cells developed at the Michigan cancer Foundation were kindly provided by Dr. Robert P.C. Shiu (University of Manitoba, Winnipeg, Manitoba, Canada; 2012). T47D cells were purchased from the ATCC (2004). Tamoxifen (TMX)-sensitive MCF7 cells and TMX-resistant LCC2 cells were kindly provided by Dr. Janne Lehtiö (Karolinska Institutet, Stockholm, Sweden; 2012). LCC2 cells originate from MCF-7 cells. These cell lines were authenticated by short tandem repeat profiling (Uppsala Genome Center, Sweden) in June 2016. MCF7 and LCC2 cells were maintained in Dulbecco's modified Eagle's medium (DMEM) supplemented with 10% fetal bovine serum (FBS) and 1% penicillin/streptomycin (Gibco). T47D cells were grown in RPMI 1640 supplemented with 10% FBS and 1% penicillin/streptomycin. DMEM and RPMI 1640 culture medium contain 28.57 μM and 21.43 μM Cho, respectively. The content of Cho and Cho phospholipid in bovine serum is not provided by the manufacturer. No additional growth factors were added to the cell culture medium.

Chromatin immunoprecipitation followed by sequencing (ChIP-seq) or qPCR

ChIP was performed as previously described (34).

Gene expression microarray analysis

The gene expression data for MCF7 cells has been previously published (33). For T47D cells, Human Gene 2.1 ST Arrays were used for analysis of global gene expression profiling. The microarray data are deposited in GEO (accession number GSE36683 and GSE74034 for MCF7 and T47D cells, respectively).

GO analysis and identification of enriched pathways were performed using the WEB-based GEne SeT AnaLysis Toolkit.

NMR spectroscopy

Water soluble metabolites were extracted using ethanol. NMR spectra were recorded on a Bruker Avance III 600 MHz spectrometer. A multivariate comparison of metabolic profiles from estrogen-stimulated and control cells was performed using partial least squares discriminant analysis (PLSDA) on Pareto-scaled NMR spectra using PLS_Toolbox v7.5.2 (Eigenvector Research Inc.). This technique identifies linear combinations of metabolic features referred to as latent variables (LVs) that discriminates between classes of samples. Quantification was performed by binning spectral regions containing signals from identified metabolites. To aid in the identification of these metabolites, Chenomx NMR suite v7.7 (Chenomx Inc.) was used. Additionally, various 2D NMR spectra (HSQC, HMBC, COSY, TOCSY) were recorded to assure identification.

Tissue Microarray Array (TMA) analysis

CHPT1 expression in human breast cancers was analyzed in tissue microarrays (US BioMax BR1503d) by IHC. Anti-CHPT1 antibody was from The Human Protein Atlas.

Zebrafish metastatic model

TMX-sensitive MCF7 cells and TMX-resistant LCC2 cells were used. The zebrafish metastatic model was established as previously described (35).

Results

A core set of direct ERα-regulated genes in ERα+ breast cancer cells

To identify a core set of direct ERα-regulated genes, we combined genome-wide ERα binding profiles with detailed transcript profiling for the two breast cancer cell lines, MCF7 and T47D. 18040 and 12659 ERα binding regions were identified for MCF7 cells and T47D cells,

respectively (Fig. 1A). General properties of the identified ERα binding regions, such as peak distribution and enriched motifs, are consistent with previously published studies (Supplementary Fig. 1A-C). Overlaying the MCF7 and T47D cistromes revealed 6480 shared binding regions, corresponding to 36% and 51% of the MCF7 and T47D cistromes, respectively (Fig. 1A and 1B). The shared binding regions overlapped with published ERα cistromes for breast cancer cell lines (Supplementary fig. 1D).

Global gene expression profiling revealed 2531 and 1800 estrogen regulated genes in MCF7 and T47D cells, respectively (Fig. 1C). Overlaying the estrogen regulated MCF7 and T47D transcriptomes identified 420 common estrogen induced and 348 common estrogen repressed genes (Fig. 1C). ERα binding was enriched in regions associated with estrogen induced genes as compared to repressed genes for both MCF7 and T47D cells (Fig. 1D). To further identify a core set of direct ERα target genes common to MCF7 and T47D cells, we combined genome-wide ERα binding profiles and estrogen regulated transcript profiles focusing on the 4739 ERα binding regions within 25 kb up- and down- stream of TSSs of their most proximal genes. Integrating these ERα binding regions with estrogen-regulated transcript profiling, we identified a core set of 207 direct ERα target genes (Supplementary table 1). A number of well-established direct ERα target genes were included in the identified core set, such as trefoil factor 1 (TFF1), growth regulation by estrogen in breast cancer 1 (GREB1), and progesterone receptor (PR). A majority (71%) of the core set of direct ERα target genes were induced by E2 treatment (Fig. 1E).

Gene ontology (GO) pathway analysis for the core set of direct ERα target genes showed significant enrichment of cancer pathways. Interestingly, metabolic pathways were also enriched (Fig. 1F). Overlaying the identified core set of direct ERα target genes with 1620 metabolic enzymes extracted from the KEGG database revealed that 19 genes encoding metabolic enzymes were direct ERα target genes in the two investigated cell lines, including

estrogen upregulation of ADCY9, B4GALT1, CA12, CHPT1, CHSY1, ENTNK2, FHL2, ITPK1, MBOAT1, PISD, PTGES, and SLC27A2 and estrogen downregulation of ABCC5, ABCG1, ACSL1, CYP1A1, CYP1A2, RXRA, and ST3GAL1 (Fig. 1G).

Estrogen signaling leads to global metabolic reprogramming in breast cancer cells

We determined the effect of estrogen signaling on levels of intracellular and extracellular metabolites using proton nuclear magnetic resonance (^{1}H NMR). Fig. 2A demonstrates a clear effect of estrogen signaling on the intracellular metabolic profile for both cell lines. Samples from estrogen treated cells were more separated from the control samples along LV1 for MCF7 cells compared to T47D cells, indicating a stronger metabolic response to E2 stimulation in MCF7 cells. Notably, the metabolic profiles from MCF7 and T47D cells were clearly separated along LV2 (Fig. 2A), indicating that the metabolic characteristics of MCF7 and T47D are inherently different. Quantitative analyses of the NMR spectra normalizing to protein levels are shown in Supplementary table 2. Notably, the area-normalized spectra were used for identification of changed metabolites (Supplementary table 3). For the MCF7 cell line, 29 unique metabolites were quantified. Levels of 19 of these metabolites were significantly modulated (FDR adjusted $p < 0.05$) upon estrogen treatment (Supplementary table 3, Supplementary Fig. 2A). For the T47D cell line, levels of 13 of 29 metabolites were significantly modulated upon estrogen treatment (Supplementary table 3, Supplementary Fig. 2B). All estrogen modulated intracellular metabolites, seven of which were changed in both cell lines, were mapped to metabolic pathways (Fig. 2B). Estrogen modulated amino acid synthesis in both cell lines (Supplementary Fig. 2A and 2B), resulting in increased phenylalanine, tyrosine and 1-methyl histidine levels (Fig. 2B). Additionally, estrogen modulated the Cho metabolic pathway, with PCho being reduced in both cell lines (Fig. 2B). However, we also observed differential effects of estrogen on Cho- containing metabolites

between these two cell lines, with glycerophosphocholine (GPC) levels being reduced in MCF7 cells and Cho levels increased in T47D cells (Supplementary Fig. 2A and 2B).

Analysis of extracellular metabolites revealed that upon estrogen treatment, MCF7 cells consumed more glucose and produced more lactate (Fig. 2C and 2D), leading to a higher lactate/glucose ratio (Fig. 2E). Surprisingly, T47D cells consumed significantly higher amounts of glucose than MCF7 cells regardless of estrogen treatment (Fig. 2C where the extracellular concentration of glucose is much lower for T47D cells compared to MCF7 cells). Similarly as observed for MCF7 cells, estrogen stimulation enhanced glucose consumption and the lactate/glucose ratio for T47D cells (Fig. 2C and 2E), supporting elevated aerobic glycolysis upon activation of estrogen signaling in ERα+ breast cancer cells. However, estrogen treatment did not affect lactate levels in T47D cells (Fig. 2D).

Estrogen signaling regulates transcripts and metabolites of the Cho metabolic pathway in breast cancer cells

The glycerophospholipid pathway which includes the Cho metabolic pathway was enriched for direct ERα target genes common to MCF7 and T47D cells (Fig. 1F). Specifically, of the 119 genes involved in the KEGG Homo sapiens glycerophospholipid pathway hsa: 00564 (27), 26 and 10 were regulated by estrogen in MCF7 and T47D cells, respectively (Fig. 3A). Regulation of a subset of these genes was confirmed using qPCR (Fig. 3B).

Additionally, metabolic profiling confirmed alterations in Cho metabolism in response to estrogen signaling for these two cell lines (Fig. 2B, Supplementary Fig. 2A and 2B). Figure 3C shows changes in the levels of metabolites in the Cho metabolic pathway upon estrogen stimulation. NMR metabolic profiling of polar extracts is not suitable for determination of the lipid soluble metabolite PtdCho, and CDP-Cho is present in too low concentration for detection by NMR. To obtain a more complete overview of the effects of estrogen on Cho

metabolism, we assayed these metabolites by alternative assays, i.e. PtdCho levels by PtdCho Assay Kit and CDP-Cho levels by LC-MS. We observed increased levels of CDP-Cho in MCF7 cells after estrogen stimulation, while no difference in T47D cells was observed (Fig. 3C). Interestingly, PtdCho levels were significantly increased 24 h after estrogen treatment in both MCF7 and T47D cells (Fig. 3D). Furthermore, CHPT1, the direct upstream enzyme to catalyze PtdCho synthesis, was identified as the only direct ERα target gene in the Cho pathway, which was upregulated upon estrogen stimulation in both analyzed cells (Fig. 3A, 3E and 3F).

All estrogen regulated genes and metabolites in the Cho metabolic pathway are indicated in Figure 3G. The expression of transmembrane Cho transporters, solute carrier family 44, members 1 and 2 (*SLC44A1*, *SLC44A2*) encoding CTL1 and CTL2, was reduced significantly after estrogen stimulation in MCF7 cells (Fig. 3B). The expression of *CHKB* and *CHKA*, which are responsible for Cho phosphorylation, was reduced by estrogen in MCF7 and T47D cells, respectively (Fig. 3B). Consistently, PCho levels were decreased in both cell lines (Supplementary table 4). Phospholipase A2, group VI (*PLA2G6*) was downregulated upon estrogen stimulation in MCF7 cells (Fig. 3B), which may result in decreased levels of its downstream product GPC, which is consistent with reduced GPC levels in this cell line in response to estrogen stimulation. The expression of *PLCD1* and *PLCE1* was significantly decreased in estrogen treated MCF7 cells (Fig. 3B). Another isoform of PLC, *PLCB3,* was downregulated by estrogen in T47D cells (Fig. 3B). Down-regulation of PLCs may result in less PCho production, consistent with what was observed for MCF7 and T47D cells (Supplementary table 4). However, it should be noted that changes in gene expression do not necessarily translate into changes in enzyme activity and metabolite concentrations.

GPC is formed by the deacylation of PtdCho. Elevated PCho/GPC ratio has been observed in breast cancer cell lines compared to normal breast epithelial cells (36). Furthermore, it has

been proposed that this ratio can predict on breast cancer aggressiveness (37,38). Our results show that estrogen stimulation increased the PCho/GPC ratio in MCF7 cells (Supplementary table 4). On the contrary, in T47D cells, the PCho/GPC ratio was reduced (Supplementary table 4).

Estrogen stimulation increases the activity of CCTα

CCTα is a key enzyme in the CDP-choline pathway for *de novo* PtdCho biosynthesis. This enzyme is inactivated when it is phosphorylated, and activated by a phosphatase which allows it to translocate to membranes (39). To understand whether E2 regulates CCTα activity, we investigated the cellular distribution of CCTα. Notably, CCTα expression was detected in cytosol, membrane and nuclear fractions (Fig. 4A). Interestingly, the level of CCTα was significantly decreased in the cytosol fraction, while it was increased in the membrane upon E2 stimulation in MCF7 and T47D cells (Fig. 4A), suggesting that CCTα was recruited to the membrane and activated in response to E2 treatment. However, no change of CCTα was observed in nuclear fraction upon E2 treatment (Fig. 4A). The separation of cytosol, membrane and nuclear proteins was confirmed by assaying the cytosolic proteins GAPDH and α-tubulin, the membrane associated proteins cadherin and TIM 23, and nuclear associated protein lamin (Fig. 4A).

CHPT1 is critical for estrogen induced PtdCho synthesis

E2 stimulation led to upregulation of both CHPT1 and its direct downstream metabolite PtdCho (Fig. 3B and 3D). To confirm the role of CHPT1 in estrogen regulation of PtdCho, we assayed PtdCho levels upon CHPT1 depletion with and without E2 treatment in MCF7 and T47D cells. Efficient knockdown of CHPT1 was confirmed by qRT-PCR and western blot analysis (Fig. 4B). Importantly, PtdCho levels decreased significantly after CHPT1 knockdown, supporting a critical role of CHPT1 in regulating PtdCho synthesis (Fig. 4C).

Furthermore, the effect of estrogen in promoting PtdCho synthesis was significantly reduced after CHPT1 knockdown (Fig. 4C), suggesting that estrogen induced PtdCho synthesis is dependent on CHPT1 expression. To further explore how metabolites of the Cho metabolic pathway are affected upon CHPT1 depletion, we determined levels of Cho- containing metabolites by ^{1}H-NMR in MCF7 cells upon CHPT1 depletion compared to control in the presence and absence of E2. As shown in Fig. 4D, CHPT1 depletion increased the levels of Cho, suggesting that CHPT1 contributes significantly to metabolic turnover in the Cho pathway in MCF7 cells. Interestingly, a significant reduction of the PCho/GPC ratio was observed upon CHPT1 depletion, and additionally, increase of the PCho/GPC ratio by E2 was abolished by CHPT1 depletion (Fig. 4E). This indicates that CHPT1 is a critical regulator of the PCho/GPC ratio, which previously has been suggested as a potential prognostic biomarker in breast cancer (40). To understand whether the PEMT pathway contributes to the increase in PtdCho levels, we assayed PEMT mRNA levels in response to E2 stimulation. However, the expression of PEMT was not induced by estrogen in the assayed breast cancer cell lines (Supplementary table 5).

CHPT1 increases anchorage- independent growth and proliferation of breast cancer cells

To further uncover the role of CHPT1 in ERα positive breast cancer cells, we examined anchorage-independent growth and proliferation after CHPT1 knockdown. As shown in Figures 5A and 5B, CHPT1 knockdown reduced the number of colonies of MCF7 and T47D cells in soft agar compared to the control. Furthermore, we observed that knockdown of CHPT1 decreased cell proliferation in both cell lines (Fig. 5C).

CHPT1 is overexpressed in breast cancer

To confirm CHPT1 dysregulation in breast cancer, we determined CHPT1 protein levels in tumor tissue and adjacent normal breast tissue by IHC, using tissue microarrays (TMAs) for which data was provided regarding tumor nodes and metastasis (TNM), clinical stage and pathology grade, and IHC- staining for HER-2, ER and PR. Consistent with published data by The Human Protein Atlas (http://www.proteinatlas.org/ENSG00000111666-CHPT1/tissue), we observed that almost all CHPT1 staining was localized to the cytoplasm (Fig. 5D). Although cytoplasmic staining was observed in both normal and cancerous tissue, staining was stronger for tumor tissues (Fig. 5D and 5E). Interestingly, higher CHPT1 expression was observed in ER+ breast cancer compared to ER- breast cancer (Supplementary table 6), consistent with CHPT1 being an ERα target gene. There was no significant correlation between CHPT1 expression and HER-2, TNM, clinical stage and pathology grade (Supplementary table 6).

Knockdown of CHPT1 inhibits early stage of metastasis of TMX-resistant breast cancer cells *in vivo*

To increase knowledge about the role of CHPT1 in invasion of TMX-resistant breast cancer cells, we performed transwell cell invasion assays for both TMX-sensitive MCF7 cells and TMX-resistant LCC2 cells upon CHPT1 knockdown (Fig. 6A). The invasion assay showed that LCC2 cells were more invasive than MCF7 cells (Fig. 6B). Knockdown of CHPT1 markedly inhibited invasion of both MCF7 and LCC2 cells (Fig. 6B). To further study the role of CHPT1 in regulating early stage of metastasis of TMX-resistant breast cancer cells *in vivo*, we used a zebrafish tumor model (36). Tumor-implanted fish embryos were scored for the dissemination of tumor cells at day 4 after injection. Control-siRNA-treated LCC2 cells disseminated more widespread in the fish body as compared to control-siRNA-treated MCF7 cells. Reduced dissemination of tumor cells was observed for both MCF7 and LCC2 cells after CHPT1 knockdown (Fig. 6C). Notably, a stronger suppression of invasion and

metastasis following CHPT1 depletion was found in LCC2 cells compared to MCF7 cells (Fig. 6D).

Discussion

Here, we combine global determination of ERα binding regions with global determination of estrogen induced gene expression for two breast cancer cell lines to define a set of 207 core direct ERα target genes. The two ERα+ breast cancer cell lines investigated in this study, MCF7 and T47D, represent distinct molecular backgrounds for ERα activity in breast cancer (32,41). Notably and consistent with previous findings, the number of ERα binding regions and fold induction in expression of estrogen induced genes in MCF7 cells exhibit greater sensitivity to estrogen treatment as compared to T47D cells (32,41). This may be due to differential impact of chromatin configuration (32) and/or different ERα expression levels between the cell lines (41).

The enriched pathways in the reported core set of direct ERα target genes included cancer pathways and metabolic pathways (Fig. 1F) and combined with the metabolic profiling reveal details of estrogen induced metabolic reprogramming in breast cancer cells. Metabolic profiling revealed metabolites with conserved modulation by estrogen between the analyzed cell lines, including higher uptake of glucose and elevated levels of PtdCho, tyrosine, phenylalanine and 1-methylhistidine, and decreased levels of PCho and ATP (Fig. 2B), which accounts for only 1/3 and 1/2 of E2 regulated metabolites in MCF7 and T47D cells, respectively. This complex response could be related to that the compositions of culture media, inherent metabolic characteristics (42) and E2 induced changes in gene expression differ between the two cell lines. A previous study showed that cell culture conditions, confluence, serum deprivation, and acidic extracellular pH could all affect metabolite levels (43). Furthermore, we have previously demonstrated that distinct metabolic profiles are

associated with differences in gene expression for different subtypes of breast cancer (27). However, importantly, estrogen regulated metabolites for the two breast cancer cell lines were related to four metabolic pathways, aerobic glycolysis, nucleotide and amino acid synthesis, and glycerophospholipid metabolism, suggesting that ERα activation may increase the production of metabolic intermediates for the synthesis of proteins, nucleic acids and lipids to support the rapid proliferation of cancer cells.

Alterations in membrane phospholipids are associated with malignant transformation (36), tumorigenicity (19), and metastasis (44). Interestingly, glycerophospholipid metabolism was one of the enriched pathways of direct ERα target genes, and additionally our metabolic profiling showed alterations in Cho-metabolite levels in response to estrogen signaling. We report that E2 decreased PCho levels and increased PtdCho levels in both MCF7 and T47D cells (Supplementary table 4 and Fig. 3D). E2 suppression of PCho in T47D cells is consistent with a previous report (12). Metabolite levels are regulated by rate of synthesis and consumption of the metabolite. Reduced PCho could be attributed to decreased CHK expression (Fig. 3B and Supplementary table 4), but also to increased CCTα activity leading to higher consumption of PCho for CDP-Cho synthesis (Fig. 3C and Fig. 4A). Moreover, down-regulation of PLC could also result in less PCho production (Fig. 3B). Furthermore, we could not exclude the possibility that PCho is dephosphorylated by phosphatases. However, it should be noted that the relationship between transcript levels and metabolite concentrations in the Cho pathway is highly complex and depends on several collateral biochemical reactions. Furthermore, it is difficult to correlate changes in metabolic flux through the pathway to steady-state metabolite levels. The metabolic effects of estrogen stimulation can therefore not be conclusively determined from changes in gene expression.

The activity of CHPT1 is regulated by thyroid hormone (45), and by arginosuccinate. Here we demonstrate that E2 stimulation led to upregulation of CHPT1 and increased PtdCho levels in

breast cancer cells (Fig. 3B and 3D). Notably, CHPT1 depletion not only decreased PtdCho levels, but also increased Cho levels in MCF7 cells (Fig. 4C and 4D). Accumulation of Cho may be the result of reduced flux through the pathway due to reduced CHPT1 activity. Our results suggest that CHPT1contributes to regulation of PtdCho synthesis in the context of ER signaling in breast cancer. CCT, the rate liming enzyme for PtdCho synthesis, has been reported to display increased expression in cancer (46,47). Interestingly, no induction of *PCYT*, which encodes CCT, was found upon E2 stimulation (Fig. 3G). However, E2 stimulation increased the activity of CCTα (Fig. 4A), which could result in sufficient substrate production for CHPT1 (CDP-Cho) to synthesize PtdCho (Fig. 3C). Hence, our study indicates that increased CHPT1 expression and increased CCTα activity was involved in the estrogen-induced increase in PtdCho synthesis (Supplementary table 5).

Previous studies have shown up-regulation of CHPT1 mRNA levels and activity in human breast cancer cells compared to normal mammary epithelial cells (48,49). Furthermore, the PCho/GPC ratio has been associated with malignant transformation (36,50). In agreement with this, CHPT1 knockdown reduced the PCho/GPC ratio in MCF7 cells (Fig. 4E), and decreased anchorage-independent growth (Figs. 5A and B) and proliferation of breast cancer cells (Fig 5C).

In conclusion, our study has uncovered that ERα activation reprograms metabolism in breast cancer cells. We identify ERα direct target genes by integrating global ERα chromatin binding with global estrogen regulated gene profiling. Metabolic profiling confirms functional consequences of these estrogen mediated transcriptional changes. We show, for the first time that the ERα target gene CHPT1, plays an essential role in estrogen induced increases in PtdCho levels. Furthermore, knockdown of CHPT1 reduces malignant phenotype and proliferation of breast cancer cells. Importantly, CHPT1 depletion greatly suppresses early stage of metastasis of TMX-resistant breast cancer cells *in vivo*. Mechanistically, estrogen

stimulated CHPT1 upregulation leading to increased PtdCho synthesis could contribute cell membrane synthesis (Fig. 7). Finally, as CHPT1 is overexpressed in breast cancer supports it is a potential drug target to be further investigated.

Disclosure of Potential Conflicts of interest

No potential conflicts of interest were disclosed.

Grant Support

The project was supported by Swedish Cancer Society (Cancerfonden).

Acknowledgements

We are grateful to the Bioinformatic and Expression Analysis core facility at the Karolinska Institute (http://www.bea.ki.se/) for performing the Affymetrix and ChIP-seq assays. Swedish Metabolomics Centre (www.swedishmetabolomicscentre.se) is acknowledged for the method development and analysis of CDP-Cho.

References

1. Cairns RA, Harris IS, Mak TW. Regulation of cancer cell metabolism. Nat Rev Cancer 2011;11(2):85-95.

2. Boroughs LK, DeBerardinis RJ. Metabolic pathways promoting cancer cell survival and growth. Nat Cell Biol 2015;17(4):351-9.

3. Ganapathy-Kanniappan S, Geschwind JF. Tumor glycolysis as a target for cancer therapy: progress and prospects. Mol Cancer 2013;12:152.

4. Hensley CT, Wasti AT, DeBerardinis RJ. Glutamine and cancer: cell biology, physiology, and clinical opportunities. J Clin Invest 2013;123(9):3678-84.

5. Flavin R, Peluso S, Nguyen PL, Loda M. Fatty acid synthase as a potential therapeutic target in cancer. Future Oncol 2010;6(4):551-62.

6. Galluzzi L, Kepp O, Vander Heiden MG, Kroemer G. Metabolic targets for cancer therapy. Nat Rev Drug Discov 2013;12(11):829-46.

7. Cicatiello L, Mutarelli M, Grober OM, Paris O, Ferraro L, Ravo M, et al. Estrogen receptor alpha controls a gene network in luminal-like breast cancer cells comprising multiple transcription factors and microRNAs. Am J Pathol 2010;176(5):2113-30.

8. Thomas C, Gustafsson JA. The different roles of ER subtypes in cancer biology and therapy. Nat Rev Cancer 2011;11(8):597-608.

9. Budczies J, Brockmoller SF, Muller BM, Barupal DK, Richter-Ehrenstein C, Kleine-Tebbe A, et al. Comparative metabolomics of estrogen receptor positive and estrogen receptor negative breast cancer: alterations in glutamine and beta-alanine metabolism. J Proteomics 2013;94:279-88.

10. Tang X, Lin CC, Spasojevic I, Iversen ES, Chi JT, Marks JR. A joint analysis of metabolomics and genetics of breast cancer. Breast Cancer Res 2014;16(4):415.

11. Giskeodegard GF, Grinde MT, Sitter B, Axelson DE, Lundgren S, Fjosne HE, et al. Multivariate modeling and prediction of breast cancer prognostic factors using MR metabolomics. J Proteome Res 2010;9(2):972-9.

12. Neeman M, Degani H. Metabolic studies of estrogen- and tamoxifen-treated human breast cancer cells by nuclear magnetic resonance spectroscopy. Cancer Res 1989;49(3):589-94.

13. Neeman M, Degani H. Early estrogen-induced metabolic changes and their inhibition by actinomycin D and cycloheximide in human breast cancer cells: 31P and 13C NMR studies. Proc Natl Acad Sci U S A 1989;86(14):5585-9.

14. O'Mahony F, Razandi M, Pedram A, Harvey BJ, Levin ER. Estrogen modulates metabolic pathway adaptation to available glucose in breast cancer cells. Mol Endocrinol 2012;26(12):2058-70.

15. Xu X, Gammon MD, Zeisel SH, Lee YL, Wetmur JG, Teitelbaum SL, et al. Choline metabolism and risk of breast cancer in a population-based study. Faseb J 2008;22(6):2045-52.

16. Katz-Brull R, Seger D, Rivenson-Segal D, Rushkin E, Degani H. Metabolic markers of breast cancer: enhanced choline metabolism and reduced choline-ether-phospholipid synthesis. Cancer Res 2002;62(7):1966-70.

17. Katz-Brull R, Margalit R, Degani H. Differential routing of choline in implanted breast cancer and normal organs. Magn Reson Med 2001;46(1):31-8.

18. Ackerstaff E, Glunde K, Bhujwalla ZM. Choline phospholipid metabolism: a target in cancer cells? J Cell Biochem 2003;90(3):525-33.

19. Glunde K, Bhujwalla ZM, Ronen SM. Choline metabolism in malignant transformation. Nat Rev Cancer 2011;11(12):835-48.

20. Resseguie M, Song J, Niculescu MD, da Costa KA, Randall TA, Zeisel SH. Phosphatidylethanolamine N-methyltransferase (PEMT) gene expression is induced by estrogen in human and mouse primary hepatocytes. Faseb J 2007;21(10):2622-32.

21. Glunde K, Jie C, Bhujwalla ZM. Molecular causes of the aberrant choline phospholipid metabolism in breast cancer. Cancer Res 2004;64(12):4270-6.

22. Grove RI, Schimmel SD. Effects of 12-O-tetradecanoylphorbol 13-acetate on glycerolipid metabolism in cultured myoblasts. Biochim Biophys Acta 1982;711(2):272-80.

23. Rohrschneider LR, Boutwell RK. The early stimulation of phospholipid metabolism by 12-0-tetradecanoyl-phorbol-13-acetate and its specificity for tumor promotion. Cancer Res 1973;33(8):1945-52.

24. Wertz PW, Mueller GC. Rapid stimulation of phospholipid metabolism in bovine lymphocytes by tumor-promoting phorbol esters. Cancer Res 1978;38(9):2900-4.

25. Kiss Z, Crilly KS, Anderson WH. Phorbol ester stimulation of phosphatidylcholine synthesis requires expression of both protein kinase C-alpha and phospholipase D. Biochim Biophys Acta 1998;1392(1):109-18.

26. Ting YL, Sherr D, Degani H. Variations in energy and phospholipid metabolism in normal and cancer human mammary epithelial cells. Anticancer Res 1996;16(3B):1381-8.

27. Moestue SA, Borgan E, Huuse EM, Lindholm EM, Sitter B, Borresen-Dale AL, et al. Distinct choline metabolic profiles are associated with differences in gene expression for basal-like and luminal-like breast cancer xenograft models. BMC Cancer 2010;10:433.

28. Nagai MA, Brentani MM. Gene expression profiles in breast cancer to identify estrogen receptor target genes. Mini Rev Med Chem 2008;8(5):448-54.

29. Ross-Innes CS, Stark R, Teschendorff AE, Holmes KA, Ali HR, Dunning MJ, et al. Differential oestrogen receptor binding is associated with clinical outcome in breast cancer. Nature 2012;481(7381):389-93.

30. Hurtado A, Holmes KA, Geistlinger TR, Hutcheson IR, Nicholson RI, Brown M, et al. Regulation of ERBB2 by oestrogen receptor-PAX2 determines response to tamoxifen. Nature 2008;456(7222):663-6.

31. Hua S, Kittler R, White KP. Genomic antagonism between retinoic acid and estrogen signaling in breast cancer. Cell 2009;137(7):1259-71.

32. Joseph R, Orlov YL, Huss M, Sun W, Kong SL, Ukil L, et al. Integrative model of genomic factors for determining binding site selection by estrogen receptor-alpha. Mol Syst Biol 2010;6:456.

33. Putnik M, Zhao C, Gustafsson JA, Dahlman-Wright K. Global identification of genes regulated by estrogen signaling and demethylation in MCF-7 breast cancer cells. Biochem Biophys Res Commun 2012;426(1):26-32.

34. Zhao C, Matthews J, Tujague M, Wan J, Strom A, Toresson G, et al. Estrogen receptor beta2 negatively regulates the transactivation of estrogen receptor alpha in human breast cancer cells. Cancer Res 2007;67(8):3955-62.

35. Rouhi P, Jensen LD, Cao Z, Hosaka K, Lanne T, Wahlberg E, et al. Hypoxia-induced metastasis model in embryonic zebrafish. Nat Protoc 2010;5(12):1911-8.

36. Aboagye EO, Bhujwalla ZM. Malignant transformation alters membrane choline phospholipid metabolism of human mammary epithelial cells. Cancer Res 1999;59(1):80-4.

37. Bhujwalla ZM, Aboagye EO, Gillies RJ, Chacko VP, Mendola CE, Backer JM. Nm23-transfected MDA-MB-435 human breast carcinoma cells form tumors with altered phospholipid metabolism and pH: a 31P nuclear magnetic resonance study in vivo and in vitro. Magn Reson Med 1999;41(5):897-903.

38. Stewart JD, Marchan R, Lesjak MS, Lambert J, Hergenroeder R, Ellis JK, et al. Choline-releasing glycerophosphodiesterase EDI3 drives tumor cell migration and metastasis. Proc Natl Acad Sci U S A 2012;109(21):8155-60.

39. Gibellini F, Smith TK. The Kennedy pathway--De novo synthesis of phosphatidylethanolamine and phosphatidylcholine. IUBMB Life 2010;62(6):414-28.

40. Moestue SA, Giskeodegard GF, Cao MD, Bathen TF, Gribbestad IS. Glycerophosphocholine (GPC) is a poorly understood biomarker in breast cancer. Proc Natl Acad Sci U S A 2012;109(38):E2506; author reply E07.

41. Lu M, Mira-y-Lopez R, Nakajo S, Nakaya K, Jing Y. Expression of estrogen receptor alpha, retinoic acid receptor alpha and cellular retinoic acid binding protein II genes is coordinately regulated in human breast cancer cells. Oncogene 2005;24(27):4362-9.

42. Radde BN, Ivanova MM, Mai HX, Salabei JK, Hill BG, Klinge CM. Bioenergetic differences between MCF-7 and T47D breast cancer cells and their regulation by oestradiol and tamoxifen. Biochem J 2015;465(1):49-61.

43. Delikatny EJ, Chawla S, Leung DJ, Poptani H. MR-visible lipids and the tumor microenvironment. NMR Biomed 2011;24(6):592-611.

44. Dahiya R, Boyle B, Goldberg BC, Yoon WH, Konety B, Chen K, et al. Metastasis-associated alterations in phospholipids and fatty acids of human prostatic adenocarcinoma cell lines. Biochem Cell Biol 1992;70(7):548-54.

45. Chatterjee D, Mukherjee S, Das SK. Regulation of cholinephosphotransferase by thyroid hormone. Biochem Biophys Res Commun 2001;282(4):861-4.

46. Dueck DA, Chan M, Tran K, Wong JT, Jay FT, Littman C, et al. The modulation of choline phosphoglyceride metabolism in human colon cancer. Mol Cell Biochem 1996;162(2):97-103.

47. Bell JD, Bhakoo KK. Metabolic changes underlying 31P MR spectral alterations in human hepatic tumours. NMR Biomed 1998;11(7):354-9.

48. Ghosh A, Akech J, Mukherjee S, Das SK. Differential expression of cholinephosphotransferase in normal and cancerous human mammary epithelial cells. Biochem Biophys Res Commun 2002;297(4):1043-8.

49. Akech J, Sinha Roy S, Das SK. Modulation of cholinephosphotransferase activity in breast cancer cell lines by Ro5-4864, a peripheral benzodiazepine receptor agonist. Biochem Biophys Res Commun 2005;333(1):35-41.

50. Mimmi MC, Finato N, Pizzolato G, Beltrami CA, Fogolari F, Corazza A, et al. Absolute quantification of choline-related biomarkers in breast cancer biopsies by liquid chromatography electrospray ionization mass spectrometry. Anal Cell Pathol (Amst) 2013;36(3-4):71-83.

Figure legends

Figure 1 A core set of direct ERα regulated genes in breast cancer cells. **A**, Venn diagram showing overlap of ERα cistromes between MCF7 and T47D cells. Cells were cultured in steroid depleted media and treated with 10 nM E2 or ethanol for 45 min. Genome-wide ERα binding sites were determined by ChIP-seq. **B**, Peak intensity heatmaps of ERα binding

regions in a ± 5kb, relative to the TSS, genomic window. **C,** Overlap of estrogen induced up- and down-regulated genes, respectively, for MCF7 and T47D cells. Cells were cultured in steroid depleted media and treated with 10 nM E2 or ethanol for 6 h. Estrogen stimulated gene expression was assayed by microarray analysis (n= 4 for MCF7 cells, n= 3 for T47D cells). **D,** Correlation of estrogen regulated gene expression with ERα binding intensity. Heatmaps show the expression changes of all genes which were ranked based on high to low fold change values in MCF7 or T47D cells. The line graphs represent the moving average plots (window size=100, step size=1) which were plotted as a function of average ERα binding of genes. These genes were arranged according to the heatmaps. **E,** A core set of direct ERα up- and down-regulated genes in breast cancer cells. Overlay of ERα cistromes with estrogen up- and down-regulated genes common to MCF7 and T47D cells . **F,** GO network analysis for the core set of direct ERα regulated genes. **G** , Direct ERα regulated metabolic genes. ERα binding is presented as the score obtained from peak analysis using MACS. Estrogen stimulated gene expression is illustrated as fold change (FC) of estrogen treatment vs vehicle control.

Figure 2 ERα reprograms cell metabolism. Cells were cultured in steroid depleted media and treated with 10 nM E2 or ethanol for 24 h. Intra-and extra- cellular metabolites were extracted and analyzed by ^{1}H NMR. **A,** Partial least squares discriminant analysis (PLSDA) of NMR identified intracellular metabolites in MCF7 and T47D cells. Data is plotted using two latent variables (LV1 and LV2) (n= 5). **B,** Metabolic profile of MCF7 and T47D cells in response to estrogen stimulation. Metabolites in red represent metabolic changes observed only in MCF7 cells. Metabolites in green represent metabolic changes observed only in T47D cells. Metabolites in blue represent metabolic changes observed in both MCF7 and T47D cells. Full names of the metabolites are shown in supplementary data. **C,** Decreased glucose levels in the culture medium in response to estrogen treatment for MCF7 and T47D cells. **D,** Lactate

levels in the culture medium in response to estrogen. Increased lactate levels are observed in MCF7 cells but not in T47D cells. **E,** Increased lactate/glucose ratio in the culture medium in response to estrogen treatment for MCF7 and T47D cells. **C**-**E**, Data represent mean± standard deviation (SD) (n= 5). Student t-test was used for calculation of statistical significance.

Figure 3 ERα regulates the Cho metabolic pathway. **A,** Heatmap of estrogen regulated genes in the Cho metabolic pathway for MCF7 and T47D cells, respectively. **B,** Confirmation of a subset of estrogen regulated genes in the Cho metabolic pathway using qRT-PCR for MCF7 and T47D cells, respectively. TFF1 was used as positive control for estrogen stimulated gene expression. The assay was performed in triplicates. **C,** Change of CDP-Cho level in response to estrogen treatment. **D,** Increased PtdCho levels in response to estrogen treatment for MCF7 and T47D cells. **E,** ERα binding site within the CHPT1 gene locus derived from ChIP-seq. **F,** ChIP-qPCR confirms recruitment of ERα to the CHPT1 gene. Data are presented as fold enrichment relative to IgG. **G,** Changes in gene expression levels and metabolite levels in the Cho metabolic pathway upon estrogen treatment for MCF7 and T47D cells, respectively. Gene names in red represent upregulated genes. Gene names in green represent downregulated genes. Changes in metabolite levels are indicated by arrow. Red arrows represent upregulated metabolites and green arrows represent downregulated metabolites. **C**, **D** and **F**, Data are presented as means± SD (n= 5 for C, and n= 3 for D and F)). Student t-test was used for calculation of statistical significance.

Figure 4 CHPT1 is critical for estrogen induced PtdCho synthesis. **A**, Decreased levels of CCTα in the cytosol, and increased levels of CCTα in the membrane in response to estrogen treatment in MCF7 and T47D cells. GAPDH is marker for cytosol proteins, cadherin is marker for membrane proteins, and lamin is marker for nuclear proteins. TIM23 is used as a loading control for membrane proteins. α-tubulin is used as a loading control for cytosol

proteins, and lamin is a loading control for nuclear proteins. **B,** Reduced mRNA and protein levels of CHPT1 72 hours after siRNAs knockdown. 36B4 was used for mRNA normalization, and β-actin was used as a loading control for Western blot. **C,** Estrogen treatment increases PtdCho levels dependent on CHPT1. **D,** Cho levels after CHPT1 depletion with and without E2 treatment in MCF7 cells. **E,** PCho/GPC ratio after CHPT1 depletion with and without E2 treatment in MCF7 cells. **B**, **D** and **E**, Cells were transfected with control or CHPT1 siRNA. Transfected cells were cultured in steroid depleted media and treated with 10 nM E2 or ethanol for 24 hours, after which the lipid metabolites were extracted and quantified using a PtdCho assay kit (Abcam), and the water soluble metabolites were extracted and quantified by ^{1}H-NMR. Data are presented as means± SD (n= 3). Student t-test was used for calculation of statistical significance.

Figure 5 CHPT1 knockdown inhibits anchorage-independent growth and proliferation of breast cancer cells. **A,** Decreased number of colonies upon CHPT1-knockdown as assayed by anchorage-independent growth. **B,** Quantitative analysis of the anchorage-independent assay. **C,** Inhibition of cell proliferation upon CHPT1 knockdown as assayed by the WST-1 assay. **B** and **C**, Data are presented as means± SD (n= 3). Student t-test was used for calculation of statistical significance. **D-E,** CHPT1 expression in human breast cancers was analyzed in tissue microarrays (TMA). **D,** Representative expression pattern of CHPT1 for normal tissue and breast cancer tissue. **E,** Quantification of CHPT1 IHC- staining for normal and breast cancer tissue.

Figure 6 Knockdown of CHPT1 inhibits early stage of metastasis of TMX- resistant breast cancer cells *in vivo*. **A**, Reduced mRNA and protein levels of CHPT1 96 hours after siRNA transfection. 36B4 was used for mRNA normalization, and β-actin was used as a loading control for Western blot. **B**, CHPT1 depletion reduces MCF7 and LCC2 cell invasiveness. **A** and **B**, Data are presented as means± SD (n= 3). Student t-test was used for calculation of

statistical significance. **C**, CHPT1 knockdown results in reduced dissemination of MCF7 and LCC2 cells in the zebrafish metastasis assay. Left, 48 hours post fertilization (hpf) zebrafish embryos of the Tg(fli1:EGFP)y1 strain in which blood vessel endothelial cells express EGFP (green) were injected the perivitelline space with approximately 300 DiI-labeled cells (red) transfected either with control siRNA or with siRNA complementary to CHPT1 in and imaged at 120 hpf. Regions indicated by white boxes in the upper full-embryo image were enlarged in the lower images. White arrowheads point to tumor cells. Inj.: Injection, mets: metastases. Size bars indicate 500 μm in the top image and 100 μm in the lower images. Right, quantification of the number of the cells in the region anterior to the intestine from the experiments.. Student t-test was used for calculation of statistical significance (n = 30-35 embryos). **D**, Inhibition of invasion or metatasis after CHPT1 knockdown. Data are presented as means± SD. Student t-test was used for calculation of statistical significance.

Figure 7 Proposed model for estrogen regulated CHPT1 mediated promotion of anchorage-independent growth and cell proliferation. ERα activation leads to increased CHPT1 gene expression. Overexpression of CHPT1 promotes PtdCho synthesis, which increases membrane synthesis.

Figure 1

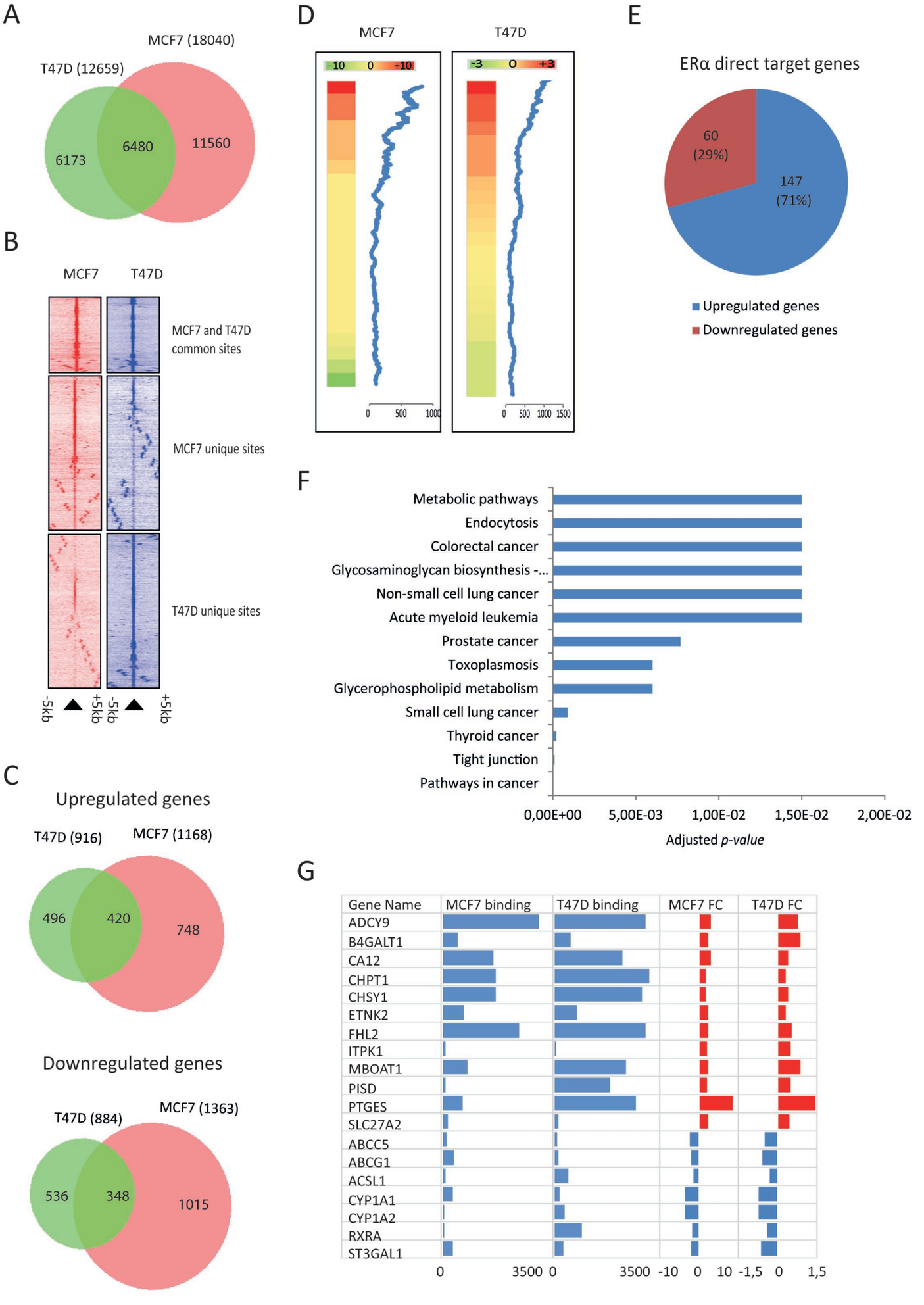
A
MCF7 (18040)
T47D (12659)
6173
6480
11560
B
MCF7
T47D
MCF7 and T47D common sites
MCF7 unique sites
T47D unique sites
-5kb
+5kb
-5kb
+5kb
C
Upregulated genes
T47D (916)
MCF7 (1168)
496
420
748
Downregulated genes
T47D (884)
MCF7 (1363)
536
348
1015
D
MCF7
T47D
-10 0 +10
-3 0 +3
0 500 1000
0 500 1000 1500
E
ERα direct target genes
60 (29%)
147 (71%)
Upregulated genes
Downregulated genes
F
Metabolic pathways
Endocytosis
Colorectal cancer
Glycosaminoglycan biosynthesis -...
Non-small cell lung cancer
Acute myeloid leukemia
Prostate cancer
Toxoplasmosis
Glycerophospholipid metabolism
Small cell lung cancer
Thyroid cancer
Tight junction
Pathways in cancer
0,00E+00
5,00E-03
1,00E-02
1,50E-02
2,00E-02
Adjusted p-value
G
Gene Name
MCF7 binding
T47D binding
MCF7 FC
T47D FC
ADCY9
B4GALT1
CA12
CHPT1
CHSY1
ETNK2
FHL2
ITPK1
MBOAT1
PISD
PTGES
SLC27A2
ABCC5
ABCG1
ACSL1
CYP1A1
CYP1A2
RXRA
ST3GAL1
0 3500 0 3500 -10 0 10 -1,5 0 1,5

Figure 2

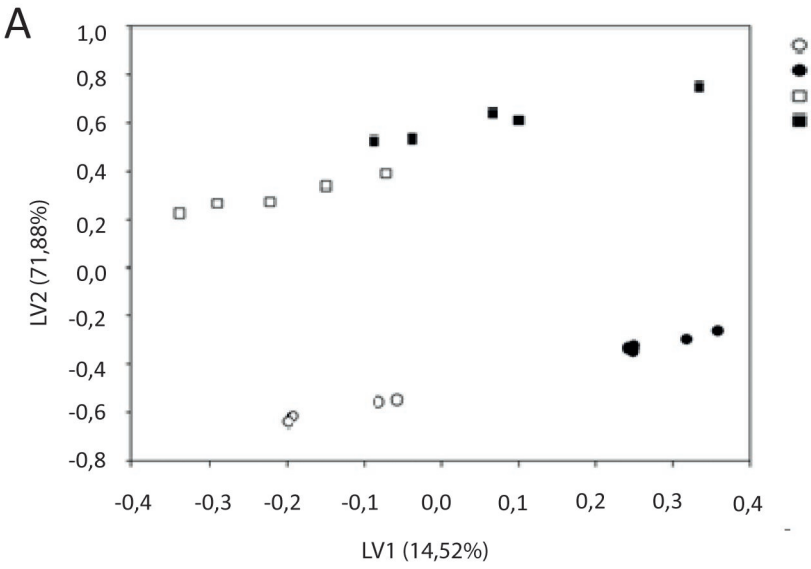
A
MCF7 ETOH
MCF7 E2
T47D ETOH
T47D E2
LV2 (71,88%)
LV1 (14,52%)

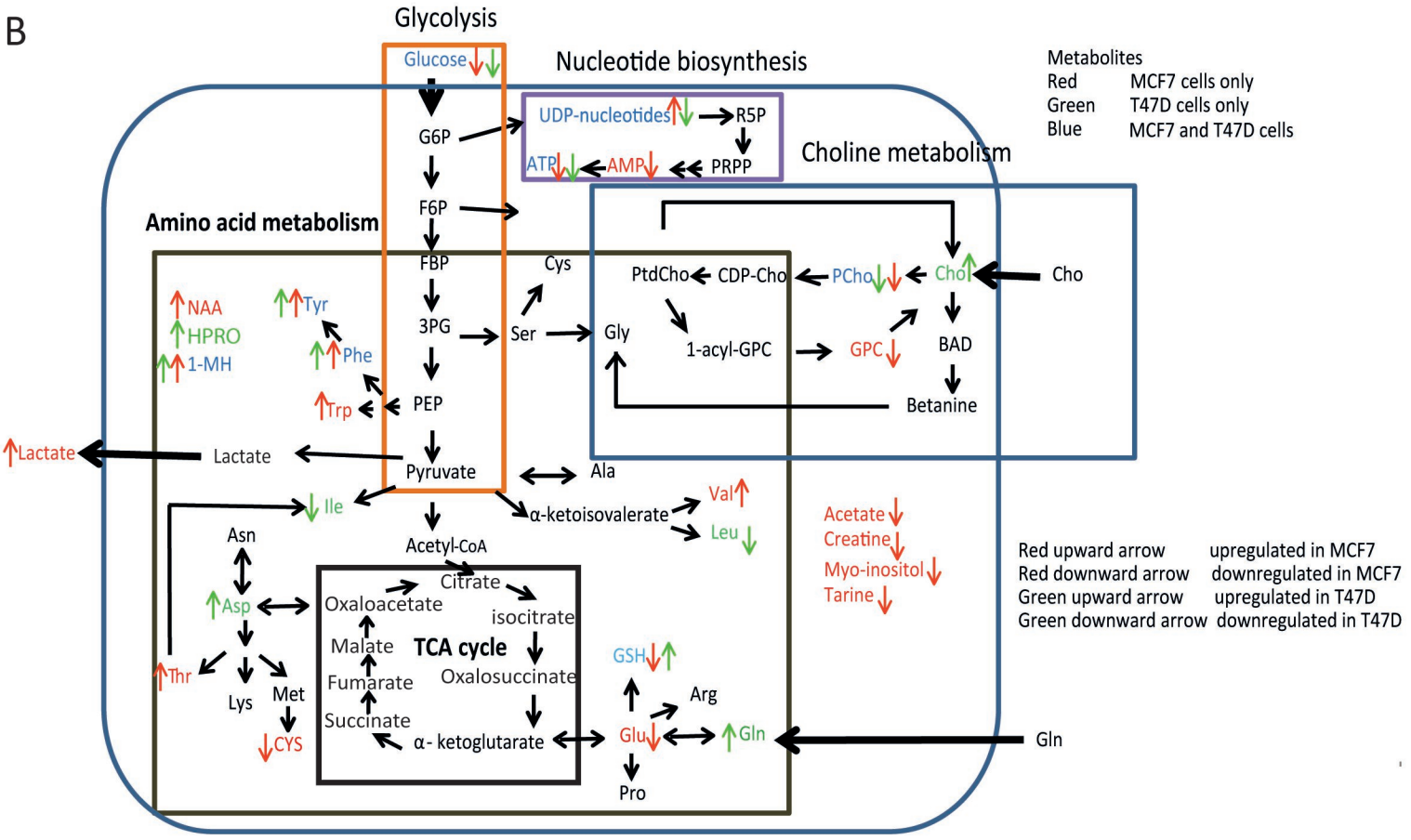
B
Glycolysis
Glucose
Nucleotide biosynthesis
UDP-nucleotides
R5P
ATP
AMP
PRPP
G6P
F6P
FBP
3PG
PEP
Pyruvate
Choline metabolism
Amino acid metabolism
Cys
Ser
Gly
Ala
PtdCho
CDP-Cho
PCho
Cho
1-acyl-GPC
GPC
BAD
Betanine
NAA
HPRO
1-MH
Tyr
Phe
Trp
Lactate
Ile
Val
Leu
α-ketoisovalerate
Acetyl-CoA
Asn
Asp
Thr
Lys
Met
CYS
Citrate
isocitrate
Oxaloacetate
Malate
TCA cycle
Fumarate
Oxalosuccinate
Succinate
α- ketoglutarate
GSH
Glu
Arg
Gln
Pro
Acetate
Creatine
Myo-inositol
Tarine
Metabolites
Red MCF7 cells only
Green T47D cells only
Blue MCF7 and T47D cells
Red upward arrow upregulated in MCF7
Red downward arrow downregulated in MCF7
Green upward arrow upregulated in T47D
Green downward arrow downregulated in T47D

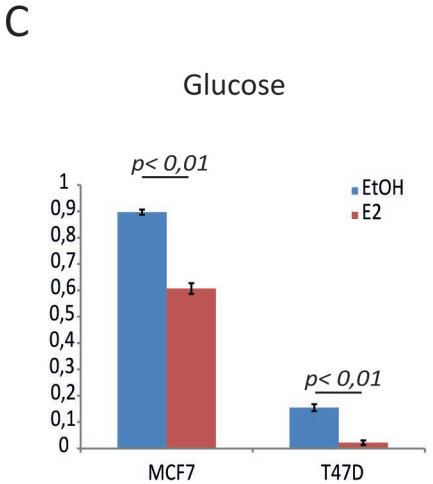
C
Glucose
p< 0,01
EtOH
E2
p< 0,01
MCF7
T47D

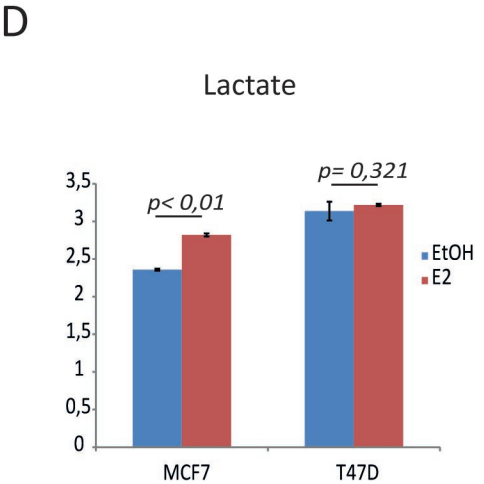
D
Lactate
p= 0,321
p< 0,01
EtOH
E2
MCF7
T47D

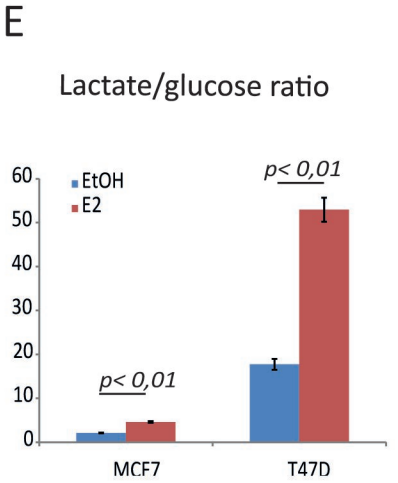
E
Lactate/glucose ratio
EtOH
E2
p< 0,01
p< 0,01
MCF7
T47D

Figure 3

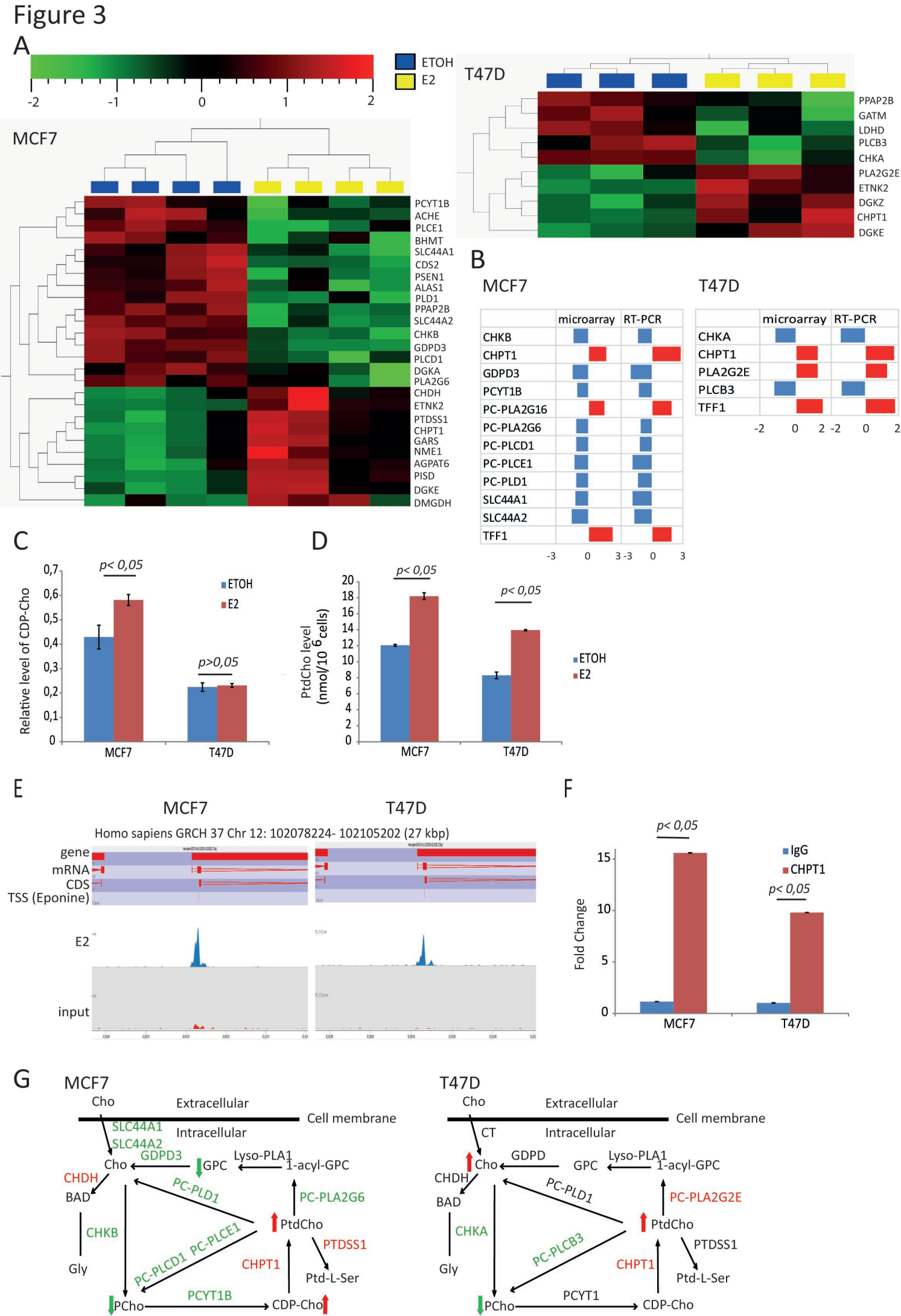
A
-2
-1
0
1
2
ETOH
E2
MCF7
PCYT1B
ACHE
PLCE1
BHMT
SLC44A1
CDS2
PSEN1
ALAS1
PLD1
PPAP2B
SLC44A2
CHKB
GDPD3
PLCD1
DGKA
PLA2G6
CHDH
ETNK2
PTDSS1
CHPT1
GARS
NME1
AGPAT6
PISD
DGKE
DMGDH
T47D
PPAP2B
GATM
LDHD
PLCB3
CHKA
PLA2G2E
ETNK2
DGKZ
CHPT1
DGKE
B
MCF7
microarray
RT-PCR
CHKB
CHPT1
GDPD3
PCYT1B
PC-PLA2G16
PC-PLA2G6
PC-PLCD1
PC-PLCE1
PC-PLD1
SLC44A1
SLC44A2
TFF1
-3
0
3
T47D
microarray
RT-PCR
CHKA
CHPT1
PLA2G2E
PLCB3
TFF1
-2
0
2
C
p< 0,05
p>0,05
ETOH
E2
Relative level of CDP-Cho
0,7
0,6
0,5
0,4
0,3
0,2
0,1
0
MCF7
T47D
D
p< 0,05
p< 0,05
PtdCho level
(nmol/10 6 cells)
20
18
16
14
12
10
8
6
4
2
0
ETOH
E2
MCF7
T47D
E
MCF7
T47D
Homo sapiens GRCH 37 Chr 12: 102078224- 102105202 (27 kbp)
gene
mRNA
CDS
TSS (Eponine)
E2
input
F
p< 0,05
p< 0,05
IgG
CHPT1
Fold Change
15
10
5
0
MCF7
T47D
G
MCF7
Cho
Extracellular
Cell membrane
Intracellular
SLC44A1
SLC44A2
GDPD3
Cho
GPC
Lyso-PLA1
1-acyl-GPC
CHDH
BAD
PC-PLD1
PC-PLA2G6
CHKB
PtdCho
PTDSS1
Gly
PC-PLCD1
PC-PLCE1
CHPT1
Ptd-L-Ser
PCho
PCYT1B
CDP-Cho
T47D
Cho
Extracellular
Cell membrane
CT
Intracellular
GDPD
Cho
GPC
Lyso-PLA1
1-acyl-GPC
CHDH
BAD
PC-PLD1
PC-PLA2G2E
CHKA
PtdCho
PTDSS1
Gly
PC-PLCB3
CHPT1
Ptd-L-Ser
PCho
PCYT1
CDP-Cho

Figure 4

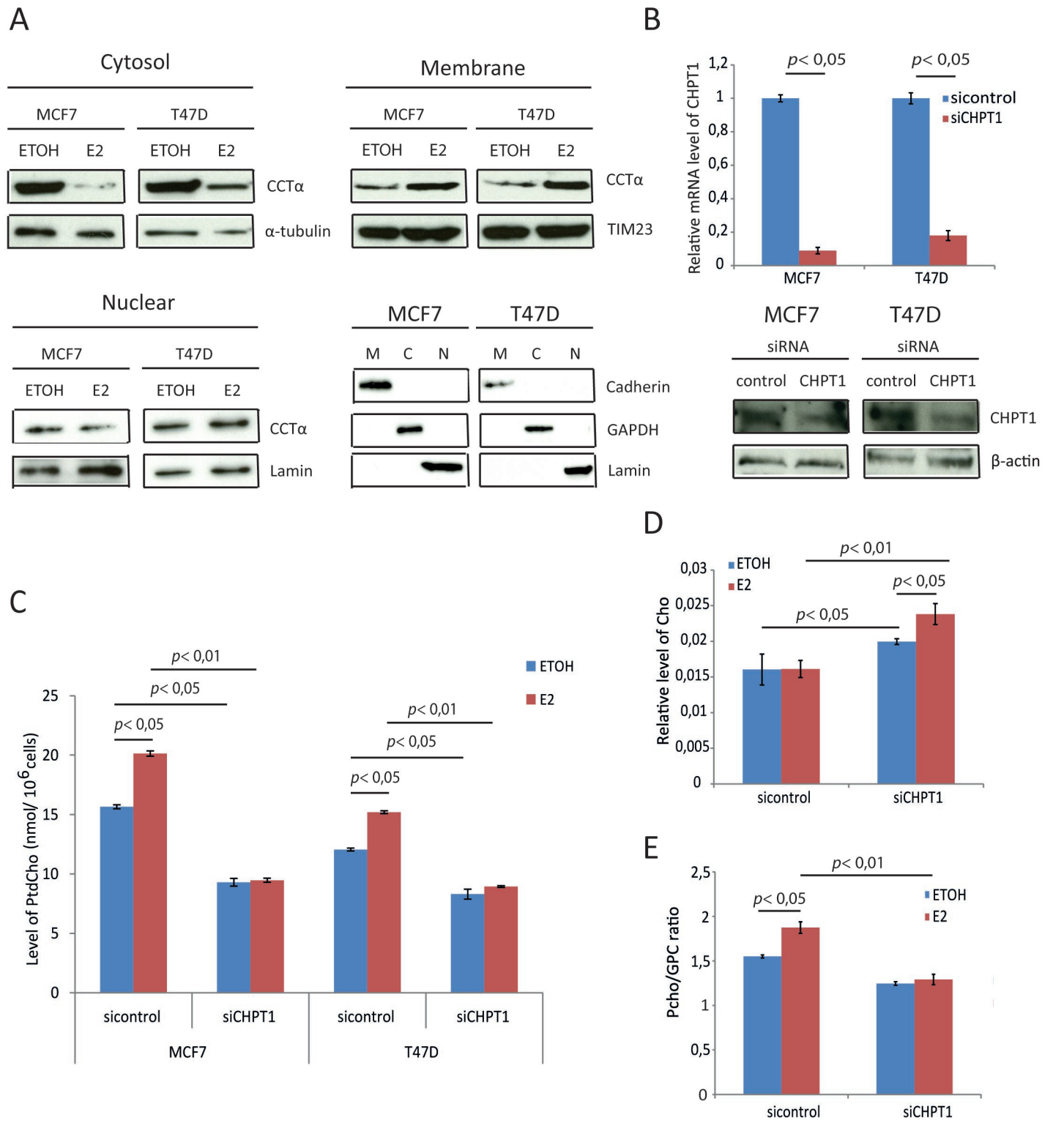
A
Cytosol
Membrane
MCF7
T47D
ETOH
E2
CCTα
α-tubulin
TIM23
Nuclear
M
C
N
Cadherin
GAPDH
Lamin
B
p< 0,05
Relative mRNA level of CHPT1
sicontrol
siCHPT1
siRNA
control
CHPT1
β-actin
C
p< 0,01
Level of PtdCho (nmol/ 10^6 cells)
D
Relative level of Cho
E
Pcho/GPC ratio

Figure 5

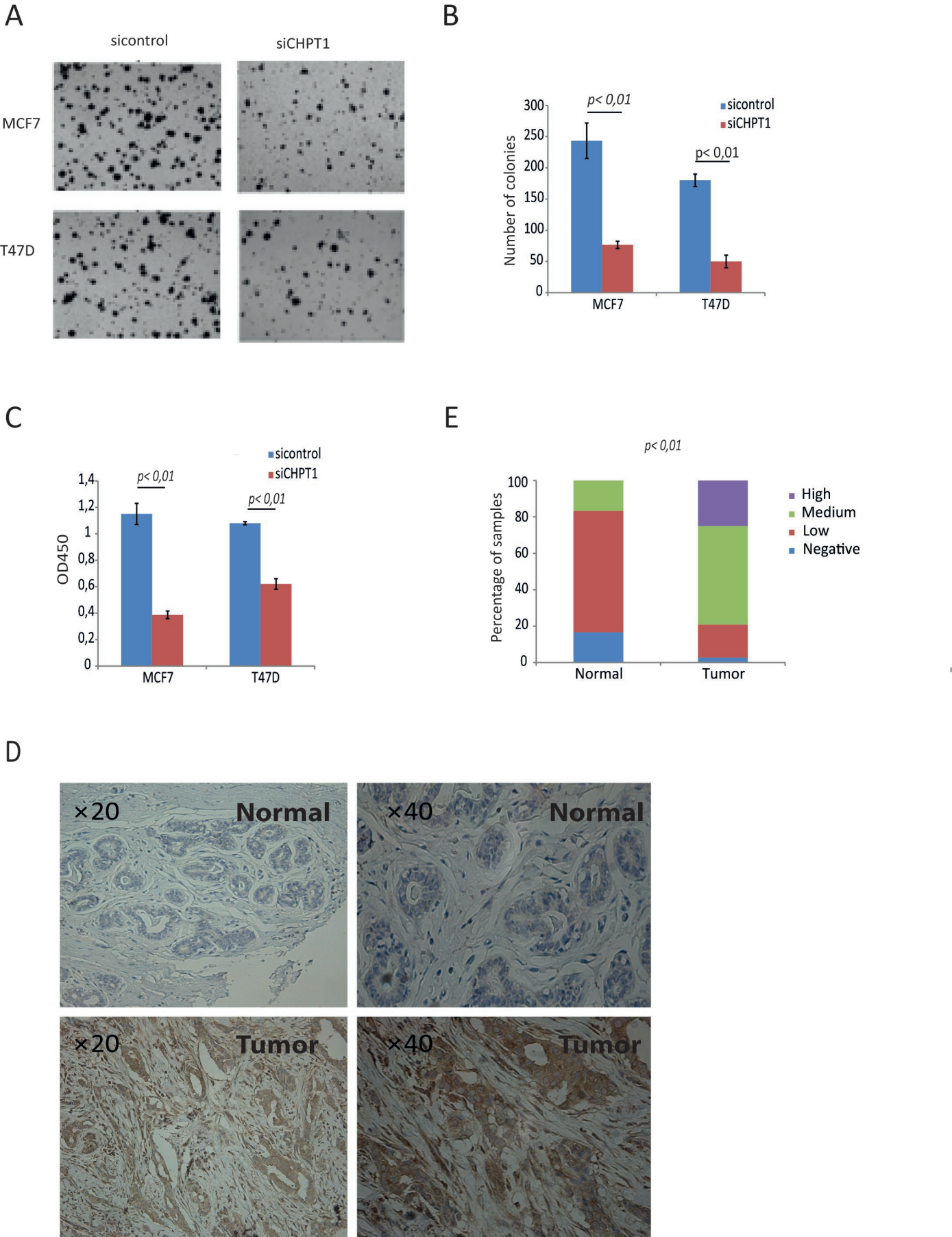
A
sicontrol
siCHPT1
MCF7
T47D
B
Number of colonies
300
250
200
150
100
50
0
p< 0,01
p< 0,01
sicontrol
siCHPT1
MCF7
T47D
C
OD450
1,4
1,2
1
0,8
0,6
0,4
0,2
0
p< 0,01
p< 0,01
sicontrol
siCHPT1
MCF7
T47D
E
p< 0,01
Percentage of samples
100
80
60
40
20
0
High
Medium
Low
Negative
Normal
Tumor
D
×20
Normal
×40
Normal
×20
Tumor
×40
Tumor

Figure 6

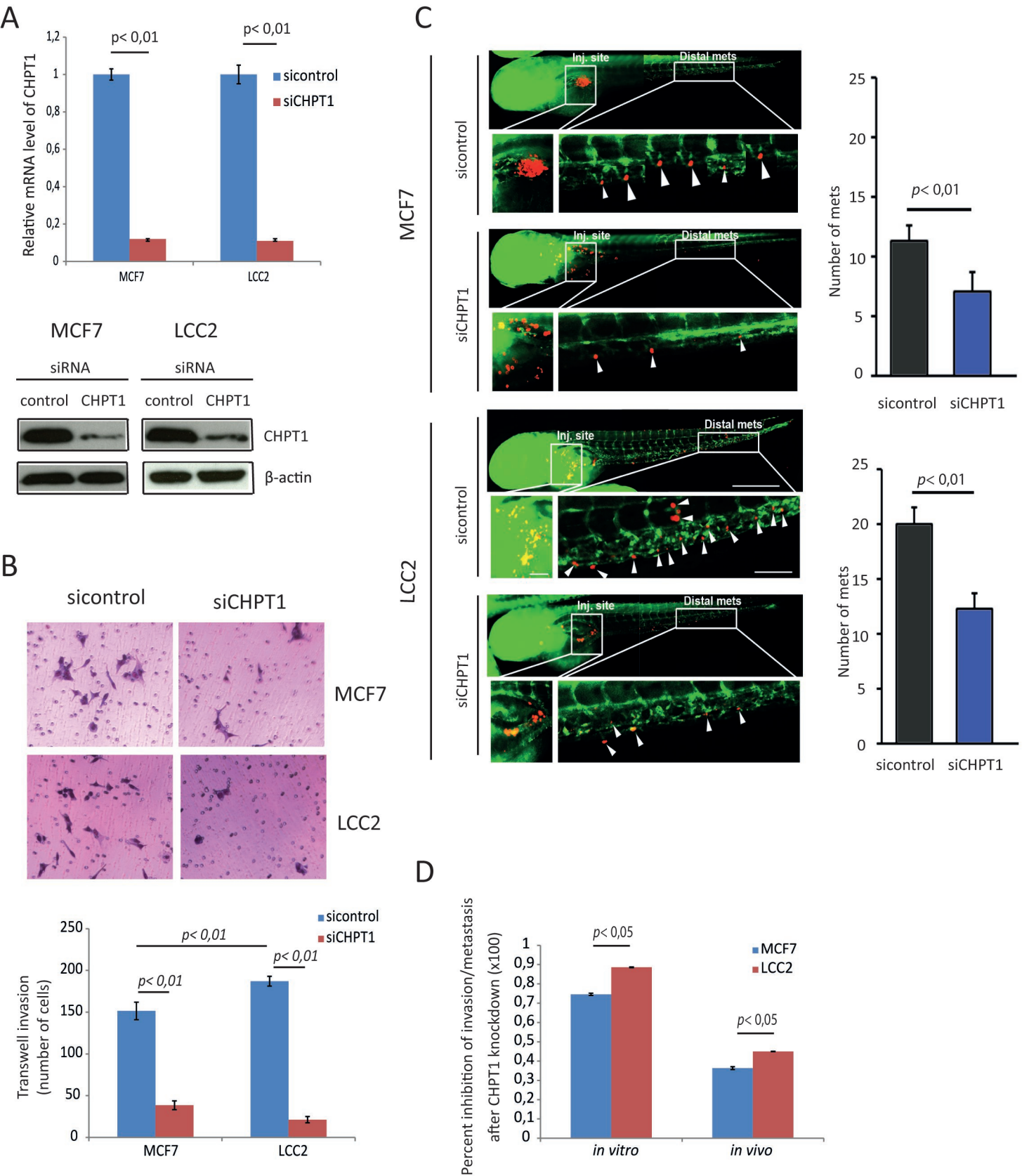
A
Relative mRNA level of CHPT1
p< 0,01
p< 0,01
sicontrol
siCHPT1
MCF7
LCC2
MCF7
LCC2
siRNA
siRNA
control
CHPT1
control
CHPT1
CHPT1
β-actin
B
sicontrol
siCHPT1
MCF7
LCC2
Transwell invasion (number of cells)
p< 0,01
p< 0,01
p< 0,01
sicontrol
siCHPT1
MCF7
LCC2
C
MCF7
LCC2
sicontrol
siCHPT1
Inj. site
Distal mets
Number of mets
p< 0,01
sicontrol
siCHPT1
D
Percent inhibition of invasion/metastasis after CHPT1 knockdown (x100)
p< 0,05
p< 0,05
MCF7
LCC2
in vitro
in vivo

Figure 7

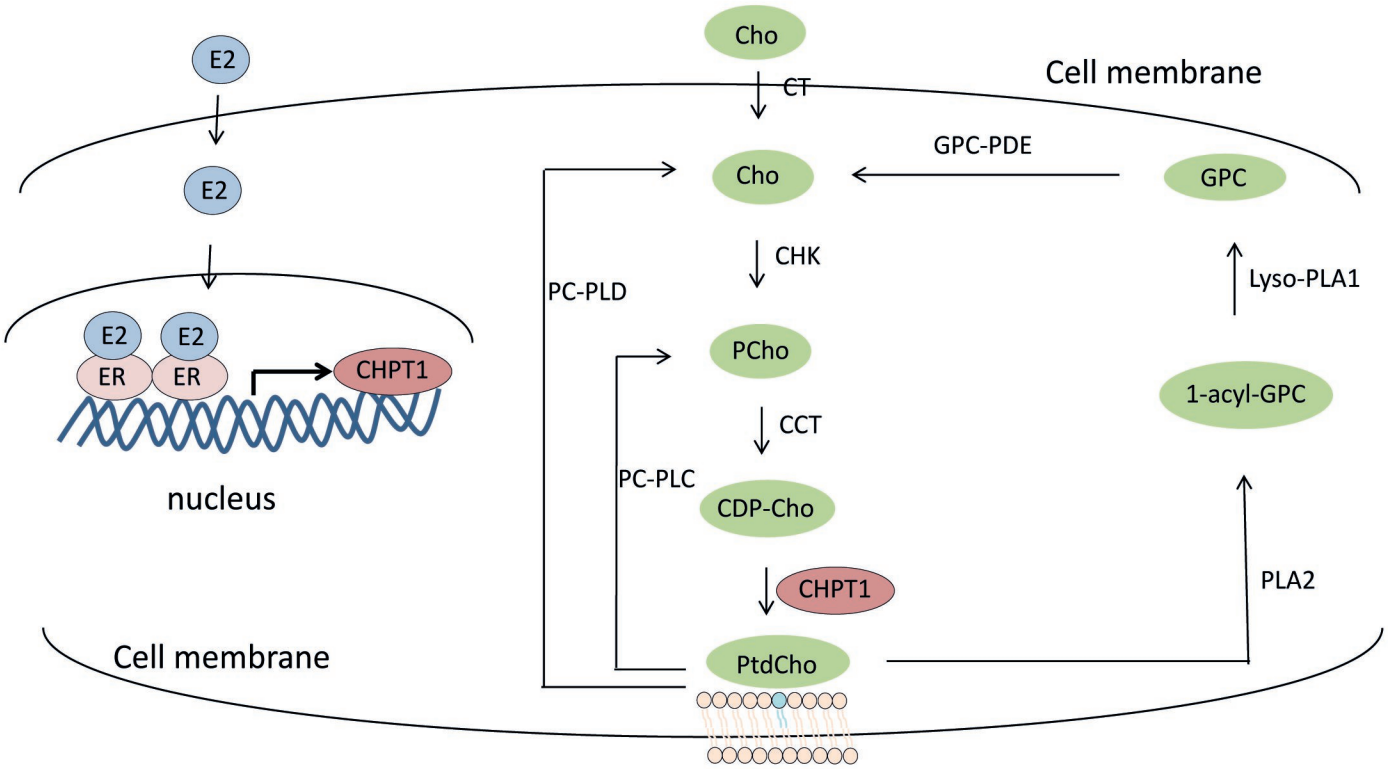
E2
E2
E2
E2
ER
ER
CHPT1
nucleus
Cell membrane
Cho
CT
Cell membrane
GPC-PDE
Cho
GPC
CHK
PC-PLD
Lyso-PLA1
PCho
1-acyl-GPC
CCT
PC-PLC
CDP-Cho
CHPT1
PLA2
PtdCho